

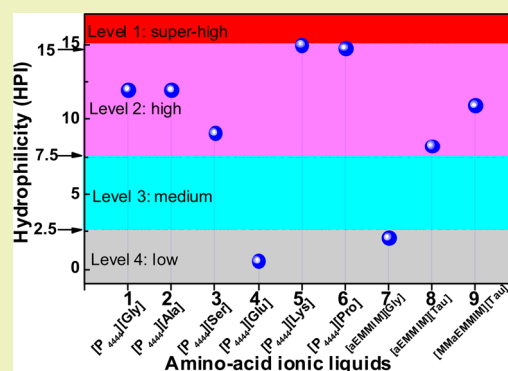
# Water Sorption in Amino Acid Ionic Liquids: Kinetic, Mechanism, and Correlations between Hygroscopicity and Solvatochromic Parameters

Yuanyuan Cao, Xiaofu Sun, Yu Chen, and Tiancheng Mu\*

Department of Chemistry, Renmin University of China, Beijing 100872, P. R. China

**ABSTRACT:** Amino acid ionic liquids (ILs) are biocompatible, biodegradable, and easy to synthesis, thus resulting in many potentially sustainable applications (e.g., sour gases capture and biomass dissolution). If mixed or contaminated with water, their properties would be altered and degradation may be induced, hence influencing their applications. Therefore, the hygroscopicity of nine amino acid ILs was investigated in this study. Furthermore, an arrow-shooting ball mechanism was proposed to simulate the interaction mechanism of water sorption. Namely, a fragile melon ILs ball would easily be split by the water arrow, i.e., a weaker cation–anion interaction induces a stronger ion–water interaction, hence producing greater hygroscopicity. Instead, a hard golden ILs ball with a higher ILs–ILs interaction would disfavor the ILs–water interaction, hence producing lower hygroscopicity. Finally, the correlations between the hygroscopicity of amino acid ILs and the solvatochromic parameters were investigated. The results showed that hygroscopicity had no direct correlation with the solvatochromic parameters, whereas it did have a close relationship with the polarity depending on the region of hydrogen-bonding basicity. Therefore, hygroscopicity could be designed by three procedures: (1) estimating the hydrogen-bonding basicity, (2) determining the region of hydrogen-bonding basicity, and (3) decreasing (increasing) the polarity, which would lead to more hydrophobic ILs in a + (–) region, where “+” and “–” indicate a positive and negative correlation between polarity and hygroscopicity parameters in a specific region of hydrogen-bonding basicity, respectively.

**KEYWORDS:** Amino acid ionic liquids, Water, Hygroscopicity, Modified two-step sorption model, Arrow-shooting ball mechanism, Solvatochromic parameters, Correlation



## INTRODUCTION

Ionic liquids (ILs) are organic molten salts with melting points at or near room temperature. They have many advantages over traditional molecular liquids, such as low vapor pressure and high thermal stability.<sup>1</sup> More importantly, the physical properties of ILs are tunable by designing the cation, anion, or both.<sup>2</sup> Low vapor pressure and high thermal stability render ILs the ability to reduce or eliminate the hazards of volatile organic compounds (VOC). Tunable physical properties make ILs useful solvents for chemical reactions, biomass dissolution, and gas capture.<sup>3–5</sup> Thus, ILs have drawn much attention in green chemistry, advanced materials, sustainable chemical engineering, etc.

The most commonly used ILs are often not environmentally friendly. For example, the hydrolysis of  $[\text{BF}_4]$ - and  $[\text{PF}_6]$ -based ILs may release toxic and corrosive HF. Accordingly, ILs composed of halogen-free groups are expected to be synthesized. One of them is amino acid ILs with amino acids as anions,<sup>6,7</sup> cations,<sup>8,9</sup> or both. Amino acid ILs are expected to be green sustainable solvents having chiral centers, biodegradable characteristics, low cost, and high biocompatibility. Particularly, amino acid ILs show potential application in many fields such as gas purification (e.g.,  $\text{CO}_2$ ,  $\text{SO}_2$ ),<sup>10,11</sup>

biomass dissolution (e.g., cellulose, chitosan),<sup>12,13</sup> separation (e.g., chiral discrimination),<sup>14</sup> and catalysts for chemical reactions (e.g., Knoevenagel condensations).<sup>15,16</sup>

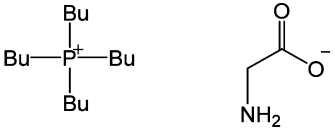
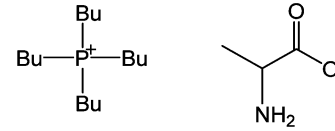
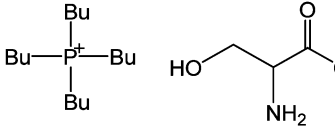
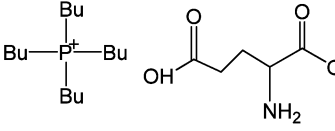
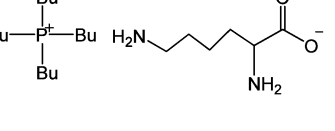
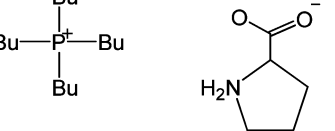
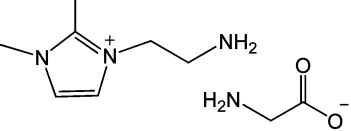
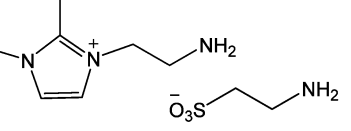
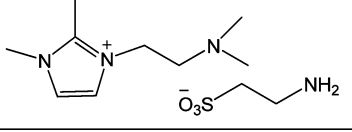
However, most ILs are hygroscopic.<sup>17–28</sup> For example, the acetate-based ILs (i.e.,  $[\text{BMIM}][\text{Ac}]$ ) could absorb 16% g/g water at  $T = 23\text{ }^\circ\text{C}$  and  $\text{RH} = 52\%$  in 3 h.<sup>17</sup> The allyl-functionalized ILs are also hygroscopic when exposed to air.<sup>20</sup> The protic ILs (i.e.,  $[\text{DEA}][\text{FO}]$ ) are more hygroscopic and could absorb as much as 25% g/g water from the air at an average  $T = 30\text{ }^\circ\text{C}$  and  $\text{RH} = 57\%$  in 24 h.<sup>23</sup> Unexpectedly, the presumed hydrophobic  $\text{Tf}_2\text{N}$ -based ILs were also found to absorb a large amount of water from a moisture environment.<sup>17,22</sup> It is inevitable for ILs to come into contact with water in the air because water is ubiquitous. The regeneration of ILs might also be very difficult after being released into a water environment, which would induce water pollution. More importantly, the presence of water could have a significant effect on the chemical structure (e.g., aggregation, intramolecular hydrogen bonding),<sup>29–31</sup> physical properties (e.g.,

Received: April 29, 2013

Revised: September 24, 2013

Published: October 2, 2013

Table 1. Name, Structure, Molar Weight of Nine Amino Acid ILs

no. of ILs	Full Name	Abbreviate Name	Chemical Structure	Molar Weight / g/mol
1	tetrabutylphosphonium glycinate	[P <sub>4444</sub> ][Gly]		333.49
2	tetrabutylphosphonium alaninate	[P <sub>4444</sub> ][Ala]		347.52
3	tetrabutylphosphonium serinate	[P <sub>4444</sub> ][Ser]		363.52
4	tetrabutylphosphonium glutamate	[P <sub>4444</sub> ][Glu]		405.54
5	tetrabutylphosphonium lysinate	[P <sub>4444</sub> ][Lys]		404.61
6	tetrabutylphosphonium prolinat	[P <sub>4444</sub> ][Pro]		374.56
7	1-aminoethyl-2,3-dimethylimidazolium glycinate	[aEMMIM][Gly]		214.26
8	1-aminoethyl-2,3-dimethylimidazolium taurinate	[aEMMIM][Tau]		264.34
9	1-(N,N-dimethyl)aminoethyl-2,3-dimethylimidazolium taurinate	[MMaEMMIM][Tau]		292.40

viscosity, density, volume, surface tension),<sup>32</sup> and industrial applications (e.g., CO<sub>2</sub> capture, cellulose dissolution) of ILs.<sup>33–35</sup>

The investigations above gave us a fundamental knowledge on water sorption by the ILs, but there has been very limited corresponding research on the hygroscopicity of amino acid ILs.<sup>36,37</sup> For the amino acid ILs, the presence of water also has a significant influence on their physical properties,<sup>38–40</sup> chemical structure, and applications.<sup>11,36,37</sup> For example, the presence of 1 wt % water could change the reaction mechanism between

amino acid ILs and CO<sub>2</sub> and hence enhance the capacity from 1:2 mol CO<sub>2</sub>/IL to 1:1 mol CO<sub>2</sub>/IL.<sup>11</sup> Another example is that only a small amount of moisture (5 mol %) could increase the efficiency of CO<sub>2</sub> permeabilities in the amino acid ILs [P<sub>4444</sub>][Gly] and [Emim][Gly] by about 1.4 and 2 times, respectively.<sup>36</sup>

As to ways to correlate or predict the hygroscopicity of ILs, several reports are listed below. Arellano et al. studied the moisture sorption kinetics of [BMIM][Br] and [OMIM][Br]. They found that the data could be favorably fitted with the

**Table 2. Water Sorption Capacity (C), Average Rate (AR), Initial Rate (IR), and Degree of Difficulty to Reach Equilibrium (D) of Amino Acid ILs<sup>a</sup>**

no.	ILs	M.W. (g/mol)	sorption capacity, $W_{\infty}$ (wt %)	sorption rate		sorption difficulty, $1/k$ (h)	$R^2$
				$kW_{\infty}$ (initial) (%/h)	$R_{24h}$ (average) (wt %/h)		
1	[P <sub>4444</sub> ][Gly]	333.49	12.00	0.53	0.31	22.66	0.9962
2	[P <sub>4444</sub> ][Ala]	347.52	11.96	0.93	0.66	12.90	0.9961
3	[P <sub>4444</sub> ][Ser]	363.52	9.08	0.79	0.02	11.49	0.9900
4	[P <sub>4444</sub> ][Glu]	404.54	0.56	0.13	0.42	4.42	0.9793
5	[P <sub>4444</sub> ][Lys]	404.61	15.00	2.37	0.07	6.33	0.9103
6	[P <sub>4444</sub> ][Pro]	374.56	14.75	0.35	0.33	42.08	0.9932
7	[aEMMIM][Gly]	214.26	2.10	0.13	0.32	16.02	0.9868
8	[aEMMIM][Tau]	264.34	8.23	0.86	0.26	9.59	0.9866
9	[MMaEMMIM][Tau]	292.40	10.93	0.50	0.32	21.90	0.9966

<sup>a</sup>The water sorption capacities were all expressed by the mass ratio, i.e., g/g H<sub>2</sub>O/ILs, multiplied by 100 only for a good data presentation in the table.

Weibull model at 298.15 K and 30% RH and with the Henderson–Pabis model at 358 K and 85% RH.<sup>24</sup> Carrete et al. analyzed the data of moisture adsorption by [C<sub>n</sub>MIM][BF<sub>4</sub>] ( $n = 2, 4, 6, 8$ ) using a modified version of the Brunauer–Emmett–Teller (BET) multilayer adsorption scheme.<sup>41</sup> After investigating the hygroscopicity of anhydrous ILs, Francesco et al. correlated the water sorption capacity with time using an exponential model,<sup>22</sup> while Mu et al. revised it with a modified two-step sorption mechanism.<sup>17</sup> But the relationship between hygroscopicity of amino acid ILs and solvatochromic parameters has not been investigated. Simply, solvatochromic parameters include polarity ( $E_{T30}$  or  $E_{T33}$ , the normalized form is  $E_T^N$ ); hydrogen-bonding donating ability,  $\alpha$ ; hydrogen-bonding accepting ability,  $\beta$ ; and dipolarity polarizability,  $\pi^*$ .<sup>42–45</sup> The solvatochromic parameters of ILs have been tremendously investigated.<sup>42,46–53</sup> The reason for selecting the solvatochromic parameters as the independent variable is that solvatochromic parameters could affect the mechanism and rate of chemical reaction.<sup>54,55</sup> More importantly, the solvatochromic parameters had a strong correlation with biomass (e.g., cellulose) dissolution,<sup>5,56,57</sup> CO<sub>2</sub>/CH<sub>4</sub> separation,<sup>58</sup> and acetylene solubility<sup>59</sup> in ILs.

Questions are raised. Other kinds of ILs are hygroscopic, so how about the amino acid ILs? Are there any correlations between the hygroscopicity of amino acid ILs and their solvatochromic parameters? How should hydrophobic ILs be designed? This paper mainly tries to answer the above questions about amino acid ILs, i.e., high hygroscopicity, strong indirect correlation between hygroscopicity and solvatochromic parameters, designing hydrophobic amino acid ILs by increasing the ILs–ILs interaction proposed by the arrow-shooting ball theory, or by decreasing (increasing) the polarity in the + (–) region.

Here, the hygroscopicity of nine amino acid ILs including six phosphonium ILs and three imidazolium ILs (Table 1) were investigated by exposing them to the air directly. The reason for selecting phosphonium amino acid ILs is that phosphonium ILs have good chemical and thermal stability and lower toxicity than ammonium salts. The tetrabutylphosphonium amino acid ionic liquids, [P<sub>4444</sub>][Gly], [P<sub>4444</sub>][Ala], [P<sub>4444</sub>][Ser], and [P<sub>4444</sub>][Lys]<sup>11</sup> (no. 1, 2, 3, 5, respectively, in Table 1) and dual amino acid ILs, i.e., [aEMMIM][Tau]<sup>10</sup> (no. 8 in Table 1) were synthesized according to the literature. In this study, we first discussed the hygroscopicity of nine amino acid ILs and regressed with a modified two-step water sorption model. Then a new arrow-shooting ball mechanism was proposed to well

interpret the water–ILs interaction. Finally, the hygroscopicity of amino acid ILs and their solvatochromic parameters were correlated.

## EXPERIMENTAL SECTION

**Materials.** All nine amino acid ILs (Table 1) were synthesized by ourselves. The six phosphonium-based amino acid ILs ([P<sub>4444</sub>][Gly], [P<sub>4444</sub>][Ala], [P<sub>4444</sub>][Ser], [P<sub>4444</sub>][Glu], [P<sub>4444</sub>][Lys], and [P<sub>4444</sub>][Pro]) were synthesized according to the literature.<sup>11</sup> Simply, tetrabutylphosphonium hydroxyl was first produced by transforming tetrabutylphosphonium bromide from the hydroxyl anion exchange resin, and then tetrabutylphosphonium-based amino acid ILs were obtained by mixing tetrabutylphosphonium hydroxyl directly with the corresponding amino acid. The imidazolium-based amino acid ILs ([aEMMIM][Gly], [aEMMIM][Tau], and [MMaEMMIM][Tau]) were synthesized as our previous reportings.<sup>10</sup> The process is almost the same as above except that the original materials, 1-aminoethyl-2, 3-dimethylimidazolium bromide and 1-(N,N-dimethyl)aminoethyl-2, 3-dimethylimidazolium bromide, are synthesized rather than bought. The details involved in the synthesis processes and reactants may be found in refs 10 and 11.

No impurity was detectable in the as-synthesized amino acid ILs by <sup>1</sup>H and <sup>13</sup>C NMR. Before use, the ILs samples were dried in a vacuum at 40 °C for 48 h. The water content was less than 290 ppm (by Karl Fisher, Karl Fisher ZDJ-400S, Multifunctional titrator, Beijing Xianqu Weifeng Company, Beijing, China). The halogen ion content was undetectable (AgNO<sub>3</sub> precipitation). The metal ion was less than 9 ppm (inductively coupled plasma optical emission spectrometry ICPOES with a Varian Vista MPX). The possible degradants of the amino acid ILs during the drying process was also excluded (NMR, Bruker AM 400 MHz spectrometer).

**Measurement of Water sorption.** The hygroscopicity of nine amino acid ILs was measured in a weighing room by exposing them to the moisture in the air directly within 24 h simultaneously. First, nine glass bottles (5 mL) were placed on nine analytic balances ( $\pm 0.1$  mg, Adventure AR224CN, Ohaus). After the zero setting, nine amino acid ILs (cal. 0.4 g) were placed in the nine glass bottles as distributed as possible on the bottom with a temperature ( $T$ ) and relative humidity (RH) sensor (Testo 608-H2, Germany,  $\pm 0.2$  °C  $T$ ,  $\pm 2\%$  RH) nearby. Then, the values of mass, temperature, and relative humidity could be obtained (Table 2). It is same as with our previous report.<sup>23</sup> The mass gain could thus be all attributed to water absorbed from the moisture in the air because the gas solubility in the ILs could be neglected due to the low partial pressure of these gases (e.g., CO<sub>2</sub>) or the low solubility of these gases (N<sub>2</sub> and O<sub>2</sub>).<sup>17,20,23</sup> The nearly identical NMR spectra of amino acid ILs before and after the water sorption also suggested the negligible gases absorbed from the air. The temperature and relative humidity within 24 h is 16.1 °C ( $\delta = 0.29$  °C) and 23.7% ( $\delta = 1.01\%$ ) on average, respectively, where  $\delta$  indicates the standard deviation (Figure 1). The fluctuation is so minimal that it can

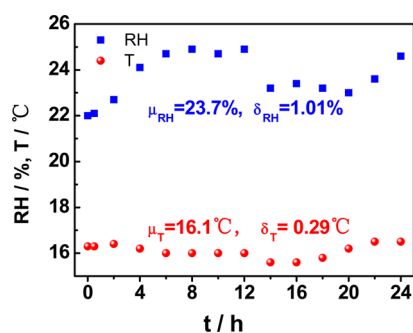
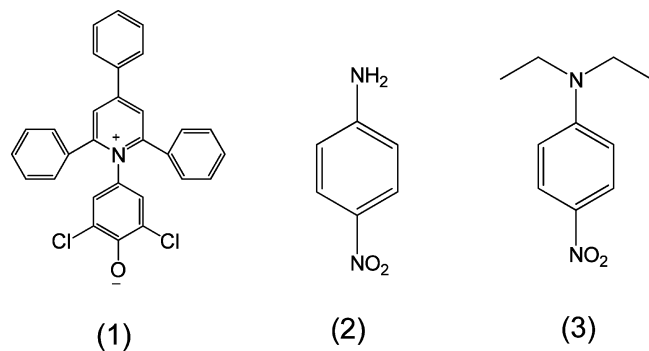


**Figure 1.** Experimental conditions of water sorption by amino acid ILs.

be neglected. The amount of water absorbed ( $W_{\text{H}_2\text{O}}$ ) is expressed as a mass ratio of water to amino acid ILs (g/g  $\text{H}_2\text{O}/\text{ILs}$ ) rather than mole ratio, so it could be compared with other reports directly due to the widespread use of mass ratio in the water sorption process.<sup>17,18,20,23,25</sup>

**Measurement of Solvatochromic Parameters.** The solvatochromic molecules (Scheme 1), Reichardt's Dye 33 (2,6-dichloro-4-

**Scheme 1. Three Kinds of Solvatochromic Probe Molecules:** 2,6-Dichloro-4-(2,4,6-triphenyl-pyridinium-1-yl)phenolate, i.e., Reichardt's Dye 33 (1), 4-Nitroaniline (2), and N,N-Diethyl-4-nitroaniline (3)<sup>a</sup>



<sup>a</sup>Probes 1, 2, and 3 measure  $\nu_{1,\text{max}}$ ,  $\nu_{2,\text{max}}$  and  $\nu_{3,\text{max}}$  with UV spectroscopy, respectively.

(2,4,6-triphenyl-pyridinium-1-yl)phenolate, probe 1), 4-nitroaniline (probe 2), and N,N-diethyl-4-nitroaniline (probe 3) were purchased from J&K Chemical Limited. The stock solution was prepared in menthol first, and then 3 or 4 drops of this stock solution were added to the glass bottle (5 mL) containing amino acid ILs. The glass bottle was placed in a vacuum for removing the solvent at 40 °C. Then, 3 wt % water was added to the glass bottle with the bottle sealed subsequently. After that, the sample in the glass bottle was mixed by

ultrasound for about 30 min. Some ILs samples were taken into a quartz cuvette (1 cm × 0.1 cm × 4.5 cm), and the UV-vis spectrum (Carry 5.0, Varian) was immediately measured. Some of the amino acid ILs (e.g., [aEMMIM][Tau]) were so viscous that the UV absorption  $\lambda_{\text{max}}$  of pure ILs could not be well detected, so 3 wt % water was added into the amino acid ILs for the determination of UV absorption  $\lambda_{\text{max}}$ . The data of solvatochromic parameters, i.e., polarity ( $E_T(33)$ ,  $E_T(30)$ ,  $E_T^N$ ), hydrogen-bonding donor ability ( $\alpha$ ), hydrogen-bonding acceptor ability ( $\beta$ ), and dipolarity polarizability ( $\pi^*$ ), could be thus derived (Table 3) from the  $\lambda_{\text{max}1}$ ,  $\lambda_{\text{max}2}$ , and  $\lambda_{\text{max}3}$  based on eqs 1, 2, 3, 4, 5, 6, 6', 7, and 7'.<sup>48,49,60</sup>

$$\nu_{\text{max}} = 10000/\lambda_{\text{max}} \quad (1)$$

$$E_T(33) = 2.859\nu_{1,\text{max}} \quad (2)$$

$$E_T(30) = 0.99382E_T(33) - 13.74797 \quad (3)$$

$$E_T^N = [E_T(30) - 30.7]/32.4 \quad (4)$$

$$\alpha = 0.0649E_T(30) - 0.72\pi^* - 2.03 \quad (5)$$

$$\nu_{2,\text{max}} = 1.035\nu_{3,\text{max}} - 2.8\beta + 2.64 \quad (6)$$

$$\beta = (1.035\nu_{3,\text{max}} - \nu_{2,\text{max}} + 2.64)/2.8 \quad (6')$$

$$\nu_{3,\text{max}} = 27.52 - 3.182\pi^* \quad (7)$$

$$\pi^* = (27.52 - \nu_{3,\text{max}})/3.182 \quad (7')$$

## RESULTS AND DISCUSSION

**Hygroscopicity.** The hygroscopicity of amino acid ILs is investigated by exposing them to air simultaneously in a weighing room. It is same as our previous report.<sup>23</sup> The average temperature is 16.1 °C, and the average relative humidity (RH) is 23.7% within 24 h, with a standard deviation of  $\delta_T = 0.29$  °C and  $\delta_{\text{RH}} = 1.01\%$ , respectively (Figure 1). The minor fluctuations of temperature and relative humidity are assumed to have a negligible effect on the data analysis.

Results show that amino acid ILs, like other ILs,<sup>17,20,22,23</sup> absorb water from the air (Figure 2). [P<sub>4444</sub>][Lys] is the most hygroscopic among the nine amino acid ILs investigated, while [P<sub>4444</sub>][Glu] is the least (Figure 2a). This indicates that the hygroscopicity of phosphonium-based amino acid ILs could be widely tuned by varying the anion, and it verifies that anions play an important role in hygroscopicity. The hygroscopicity of the three imidazolium-based amino acid ILs is among the gap of phosphonium-based amino acid ILs (Figure 2a).

[P<sub>4444</sub>][Gly], [P<sub>4444</sub>][Ala], and [P<sub>4444</sub>][Ser] differ only in the anion, with the characteristic atom of H, CH<sub>3</sub>, and CH<sub>3</sub>OH,

**Table 3.** Solvatochromic Parameters of Amino Acid ILs

no.	ILs	polarity			hydrogen-bonding donating HBD ability ( $\alpha$ )	hydrogen-bonding accepting HBA ability ( $\beta$ )	dipolarity polarizability ( $\pi^*$ )
		$E_T(33)$ (kcal/mol)	$E_T(30)$ (kcal/mol)	$E_T^N$			
1	[P <sub>4444</sub> ][Gly]	73.92	59.71	0.90	1.19	1.03	0.91
2	[P <sub>4444</sub> ][Ala]	70.42	56.24	0.79	0.99	0.84	0.87
3	[P <sub>4444</sub> ][Ser]	70.54	56.36	0.79	0.89	0.94	1.02
4	[P <sub>4444</sub> ][Glu]	70.53	56.34	0.79	0.96	0.81	0.92
5	[P <sub>4444</sub> ][Lys]	73.44	59.24	0.88	1.21	0.64	0.85
6	[P <sub>4444</sub> ][Pro]	70.96	56.78	0.80	0.98	0.99	0.94
7	[aEMMIM][Gly]	70.75	56.57	0.80	1.01	0.86	0.87
8	[aEMMIM][Tau]	68.04	53.87	0.72	0.91	0.88	0.77
9	[MMAEMMIM][Tau]	71.18	56.99	0.81	1.13	0.53	0.75

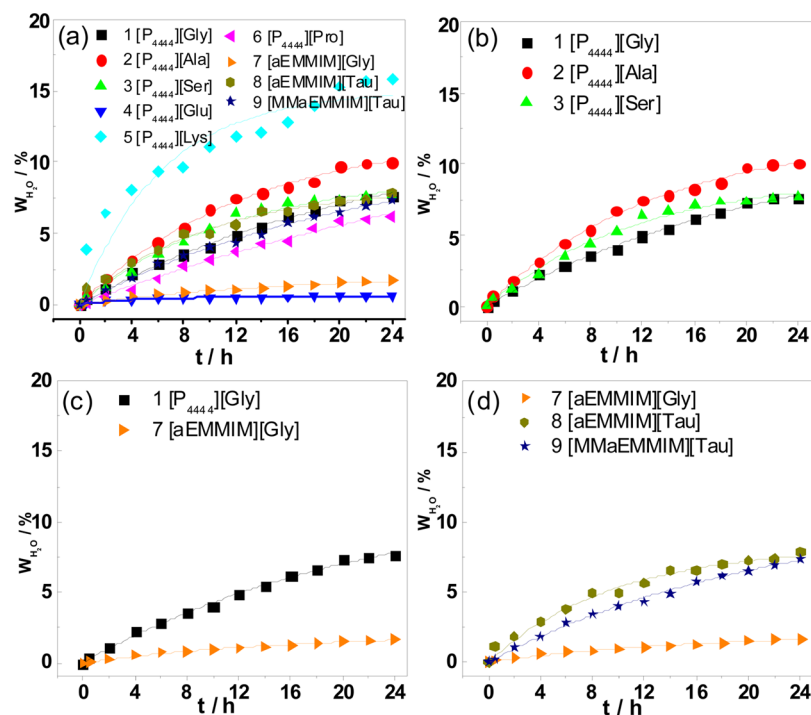


**Figure 2.** Experimental results of water sorption by amino acid ILs. Overview of nine amino acid ILs (a). Effect of methyl and hydroxyl with the amino anion (b). Effect of cation with the anion Gly (c). Effect of cations with the anion Tau (d). Fitted curves were conducted by the modified two-step sorption model<sup>17,20,23</sup> using the colored solid line to guide the eye.

respectively (Table 1), so they can be used to investigate the effect of substitution of the anion on the hygroscopicity of amino acid ILs. Figure 2b shows that  $[P_{4444}][Ala]$  with  $CH_3$  is more hygroscopic than  $[P_{4444}][Gly]$ . This might be due to the reduction of ILs–ILs interaction in the absence of H for  $[P_{4444}][Ala]$ . Note that in the case of the phosphonium-based amino acid ILs, ILs–ILs interaction mainly includes the anion–anion interaction because it is difficult for the cation  $P_{4444}$  to form hydrogen bonding with the anion. The H in  $[P_{4444}][Gly]$  enhances the hydrogen-bonding interaction of ILs–ILs and hence prevents the hydrogen-bonding interaction of ILs–water. This is consistent with Brennecke’s conclusion that a higher IL–ILs interaction for  $[OHemim][TFA]$  rather than  $[emim][TFA]$  (demonstrated by the CHELPG partial charges) results in less of a  $[OHemim][TFA]$ –water interaction (demonstrated by a more positive value of excess enthalpy  $H^E$ ).<sup>61</sup> Similarly, adding an OH in the anion for  $[P_{4444}][Ser]$  also hinders the hygroscopicity when compared to  $[P_{4444}][Ala]$  with a  $CH_3$  in the anion (Figure 2b). This again corroborates the assumption that strong ILs–ILs interaction prevents the ILs–water interaction. Another statement was also proposed by Tran<sup>21</sup> that higher amounts of water absorbed by ILs indicated a stronger water–anion (of ILs) interaction. Welton<sup>19</sup> concluded that ILs mainly interacted with the anion rather than the cation of ILs. This might also hold true for the interaction between amino acid ILs and water, i.e., water mainly interacts with the anion of amino acid ILs, and the water–anion interaction is ordered as Ala (with  $CH_3$ ) > Ser (with  $CH_3OH$ ) > Gly (with H).

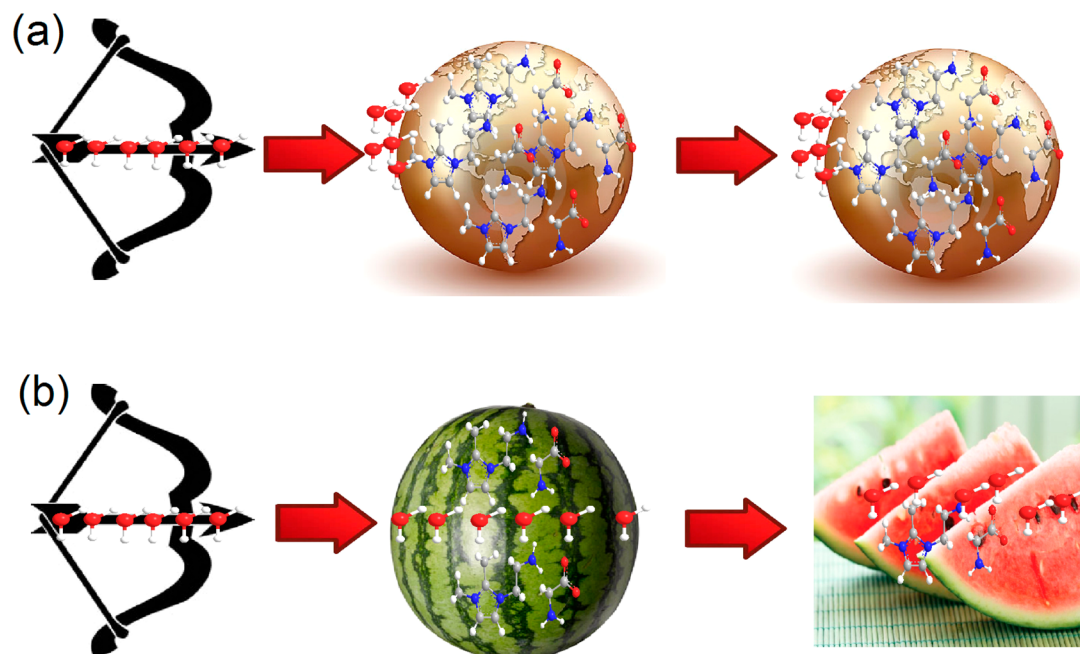
The effect of cation type was also studied by selecting  $[P_{4444}][Gly]$  and  $[aEMMIM][Gly]$ . Figure 2c shows that  $[P_{4444}][Gly]$  is more hygroscopic than  $[aEMMIM][Gly]$ . Within 24 h at  $T = 16.1^\circ C$  and  $RH = 23.7\%$ ,  $[P_{4444}][Gly]$  absorbs 7.62 wt % (mass ratio) water from the moisture in the

air, about five times greater than that of  $[aEMMIM][Gly]$  (1.66 wt %) (Table 2). This may be ascribed to the greater cation–anion interaction for  $[aEMMIM][Gly]$  due to C4H, C5H, and  $NH_2$  in the imidazolium cation. Greater cation–anion interaction takes up the position (i.e., C4H, C5H, and  $NH_2$  in the cation and anion, and COO in the anion), which is needed for the water attack. Therefore,  $[aEMMIM][Gly]$  presents less hygroscopicity than  $[P_{4444}][Gly]$ . A cation–anion hydrogen-bonding interaction (e.g.,  $[aEMMIM][Gly]$ ) may induce a stronger anti-hygroscopicity effect than an anion–anion hydrogen-bonding interaction (e.g.,  $[P_{4444}][Gly]$  and  $[P_{4444}][Ser]$  above).

$[MMaEMMIM][Tau]$  and  $[aEMMIM][Tau]$  both have an imidazolium type of cation but with a different substitute. *N,N*-Dimethylation IL  $[MMaEMMIM][Tau]$  first absorbs less water within 24 h, and after 24 h, it absorbs more water than the non-methylation counterpart  $[aEMMIM][Tau]$  (Figure 2d). The plausible explanation is that in the first 24 h viscosity dominates the hygroscopicity. The viscosity of  $[MMaEMMIM][Tau]$  with *N,N*-dimethylation is higher than that of  $[aEMMIM][Tau]$ , so less water is absorbed. However, after 24 h, the cation–anion interaction dominates the hygroscopicity. The greater interaction between the cation–anion for  $[aEMMIM][Tau]$  with  $NH_2$  leads to less interaction between the cation–water and anion–water, producing less hygroscopicity.

$[aEMMIM][Gly]$  and  $[aEMMIM][Tau]$  have the same cation but a different anion, so  $[aEMMIM][Tau]$  is more hygroscopicity (Figure 2d). The reason might be that Gly with the COO group is more hydrophilic than Tau with the  $SO_3$  group, thus Gly could interact with the cation more strongly by hydrogen-bonding with C4H and C5H rather than  $SO_3$ . Similar to our above analysis, the greater interaction between the cation–anion (i.e.,  $[aEMMIM][Gly]$ ) disfavors the interaction

Scheme 2. Proposed arrow-shooting ball interaction mechanism between amino acid ILs (ball) and water (arrow). When the arrow shoots a higher ILs–ILs interaction (i.e., hard golden ball), there is lower hygroscopicity (a). When the arrow shoots a lower ILs–ILs interaction (i.e., fragile melon ball), there is a higher hygroscopicity (b).



between the cation–water and anion–water, producing less hygroscopicity.

**Arrow-Shooting Ball Mechanism.** The above discussion suggests that a greater ILs–ILs interaction results in less ILs–water interaction, producing less hygroscopicity. An arrow-shooting ball mechanism is proposed to understand this interaction process vividly (Scheme 2). Briefly, the arrow and ball represent water and IL, separately. The interaction between the ILs–water resembles a water arrow shooting an amino acid ILs ball. If the ILs ball is hard enough (i.e., golden ball), the interaction between IL–IL is strong, and the water arrow is difficult to shoot through (Scheme 2a). In this case, the interaction between the ILs and water would not be strong, hence producing less hygroscopicity. On the contrary, the fragile ILs ball (i.e., melon ball) could be easily attacked by the water arrow, thus producing a greater interaction between the ILs and water (i.e., high hygroscopicity) (Scheme 2b).

The hard golden ball with greater ILs–ILs interactions includes two cases: greater anion–anion interaction (e.g., [P<sub>4444</sub>][Ser]) and greater cation–anion interaction (e.g., [aEMMIM][Gly]). The first case mainly refers to the cation without the ability to form hydrogen-bonding with an anion, such as phosphonium. Instead, the imidazolium cation, as in the second case, could form strong hydrogen-bonding with an anion by C4H, C5H, or C2H (if possible).<sup>29–31,62</sup> Both cases (in hard ball) lead to an unfavorable interaction between ILs and water, producing less hygroscopicity of the corresponding amino acid ILs, when compared to that of the fragile melon ball.

This indicated that functionalization of ILs did not necessarily lead to a higher hygroscopicity than that of the nonfunctionalized counterpart. It might be very helpful to design hydrophobic ILs with functionality in some specific position. Brennecke also concluded that hydroxyl functionalized on the imidazolium cation (1-(2-hydroxyethyl)-3-methylimidazolium trifluoroacetate) is more hydrophobic

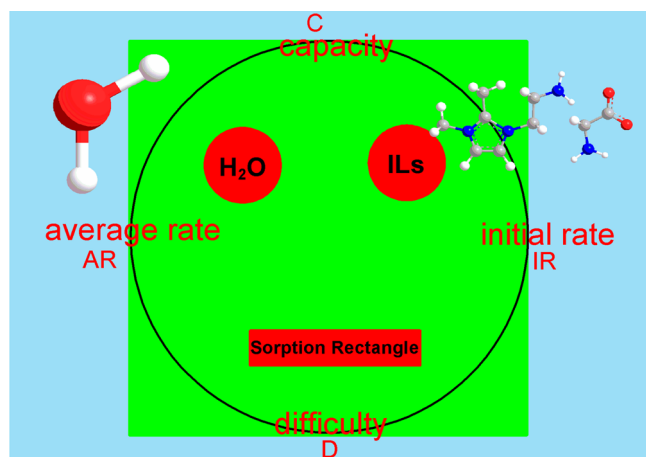
than the non-hydroxyl counterpart (1-ethyl-3-methylimidazolium trifluoroacetate).<sup>61</sup> Whereas our previous investigation showed that allyl-functionalization would enhance the hygroscopicity of ILs.<sup>20</sup>

**Sorption Rectangle.** On the basis of our previous proposed modified two-step sorption model  $W = W_{\infty}(1 - e^{-kt})$ ,<sup>17,20,23</sup> sorption capacity ( $C$ ) is indicated by the steady-state water sorption capacity,  $W_{\infty}$ . Similarly, by the model, the average rate (AR) and degree of difficulty to reach equilibrium ( $D$ ) could be defined with the parameter  $R_{24h}$ , and  $1/k$ , respectively. Previous reports mainly focus on these three parameters, i.e., capacity, average rate, and sorption difficulty.

However, the initial rate (IR) of water sorption is also very important as far as the hygroscopicity of amino acid ILs. For example, reports showed that the presence of 1 wt % (mass fraction) water could change the reaction mechanism between amino acid ILs and CO<sub>2</sub>, and hence enhance the capacity from 1:2 mol CO<sub>2</sub>/IL to 1:1 mol CO<sub>2</sub>/IL.<sup>11</sup> In our results, we found that within 30 min the most hygroscopic amino acid IL [P<sub>4444</sub>][Lys] can absorb 3.87 g water for 100 g IL, i.e., 3.73 wt % (mass fraction) (Figure 1). [aEMMIM][Tau] could also absorb 1.11 wt % (mass fraction) water from the moisture in the air within 30 min (Figure 1). Previous reports also suggests that the water sorption within the first 30 min is significant, particularly for hygroscopic ILs (e.g., [BMIM][Ac]);<sup>17,20,23</sup> 30 min is a moderate time period.

The hint is that the initial rate (IR) of water sorption is also important. The parameter  $kW_{\infty}$  could be used as the indicator of the initial sorption rate criterion. Therefore, it could be well concluded by the water sorption rectangle (Scheme 3). Four vertexes of rectangles imply the water sorption capacity, initial rate, average rate, and sorption difficulty, respectively. This sorption rectangle (Scheme 3) connects the four criteria for assessing the hygroscopicity of ILs comprehensively and might also be useful for assessing the CO<sub>2</sub> capture or cellulose dissolution by ILs.

**Scheme 3. Water sorption rectangle for amino acid ILs:** capacity (*C*), average rate (*AR*), initial rate (*IR*), and degree of difficulty to reach equilibrium (*D*)



**Hydrophilicity.** Hydrophilicity of amino acid ILs (HPI) is evaluated by  $100 W_{\infty}$ , which is derived from the modified two-step sorption model  $W = W_{\infty}(1 - e^{-kt})$ .<sup>17,20,23</sup> Namely,  $100 W_{\infty}$  means the steady-state water sorption capacity by amino acid ILs, indicating the overall affinity of amino acid ILs with water.<sup>17,20,23</sup> According to the criteria suggested in our previous work,<sup>17,20,23</sup> the hydrophilicity of the ILs is divided into four levels: superhigh hydrophilicity (level 1,  $15 \leq \text{HPI}$ ), high hydrophilicity (level 2,  $7.5 \leq \text{HPI} < 15$ ), medium hydrophilicity (level 3,  $2.5 \leq \text{HPI} < 7.5$ ), and low hydrophilicity level (level 4,  $\text{HPI} < 2.5$ ).

Six of the nine amino acid ILs investigated have the high hydrophilicity level (level 2) by this criterion. Two of them are low hydrophilic (level 4), and one is superhighly hydrophilic (level 1) (Figure 3). It could be concluded that most of the

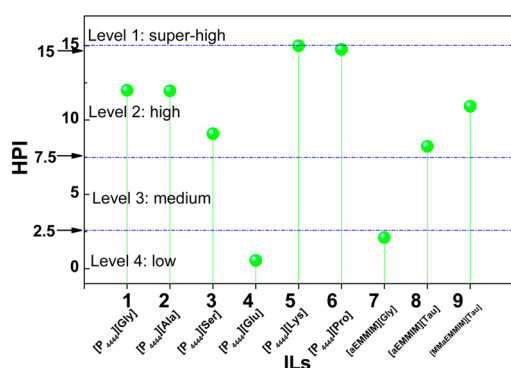


**Figure 3.** Four levels of hydrophilicity of amino acid ILs (HPI). The value of HPI is indicated by the absolute value of  $100 W_{\infty}$ .

amino acid ILs (two-thirds of the total number on average) are high hydrophilic (Figure 3). Therefore, amino acid ILs should be prohibited from contacting with water or moisture in the air in the practice. Also, removing water from amino acids should be conducted in a longer period if water has a non-negligible effect on the experimental results. Particularly,  $[P_{4444}][\text{Lys}]$  and  $[P_{4444}][\text{Pro}]$  should be paid close attention because they are very hydrophilic (Figure 3).

**Correlations between Hygroscopicity and Solvatochromic Parameters.** The hygroscopicity parameters of the amino acid ILs were also correlated with the solvatochromic

parameters. In general, the hygroscopicity parameters and solvatochromic parameters are not well directly related. For example, the correlation coefficient for  $W_{\infty}$  and  $E_T^N$  is only 0.4159 (Figure 4). However, the hygroscopicity parameters

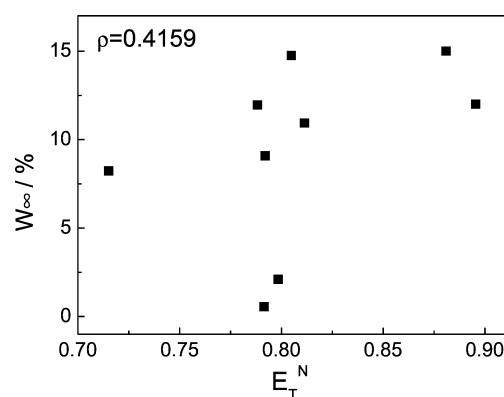


**Figure 4.** Relationship between  $W_{\infty}$  and  $E_T^N$ , with a correlation coefficient  $\rho = 0.4159$ .

have a good indirect relationship with the solvatochromic parameters, i.e., closely related to the polarity depending on the region of hydrogen-bonding basicity (Figures 5, 6, 7 and 8). This indirect relationship is expressed with the symbol “+” or “−”, which is discussed below.

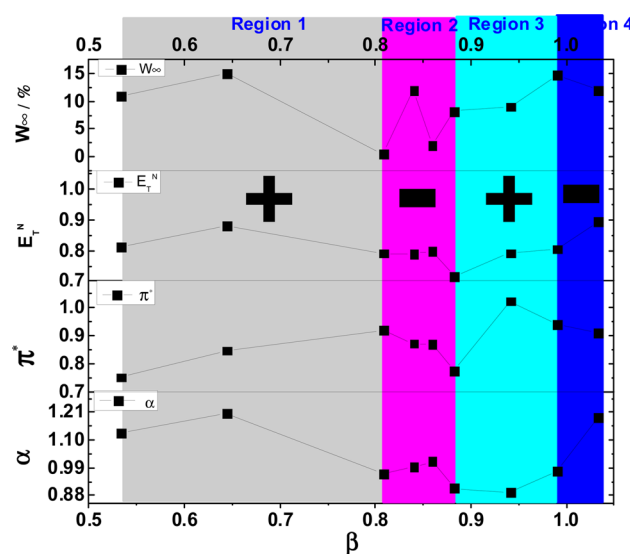


**Figure 5.** Relationship between steady-state water sorption capacity  $C$  ( $W_{\infty}$ ) and  $E_T^N$ ,  $\alpha$ ,  $\beta$ , and  $\pi^*$  of amino acid ILs.

**Water Sorption Capacity.** Water sorption capacity has always been paid close attention because it represents the overall affinity of ILs with water. The saturated water sorption capacity  $W_{\infty}$  derived from the modified two-step model,<sup>17,20,23</sup> is correlated with the four solvatochromic parameters (i.e., polarity,  $E_T^N$ ; hydrogen-bonding donating ability,  $\alpha$ ; hydrogen-bonding accepting ability,  $\beta$ ; and dipolarity polarizability,  $\pi^*$ ) (Table 3 and Figure 5). Among the parameters  $E_T^N$ ,  $E_T(33)$ , and  $E_T(30)$ , only  $E_T^N$  is chosen to analyze the data because (i) these parameters have the same tendency as stated by eqs 2, 3, and 4 and (ii)  $E_T^N$  is the normalized one with widespread usage in practice.

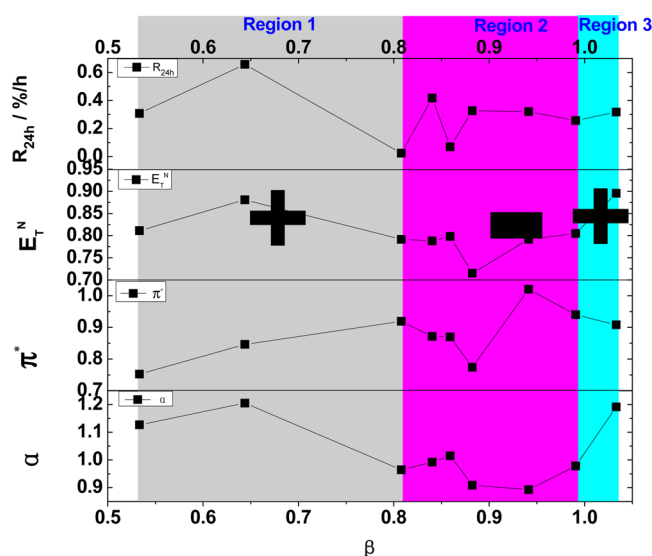


**Figure 6.** Relationship between water sorption average rate AR ( $R_{24h}$ ) and  $E_T^N$ ,  $\alpha$ ,  $\beta$ , and  $\pi^*$  of amino acid ILs.

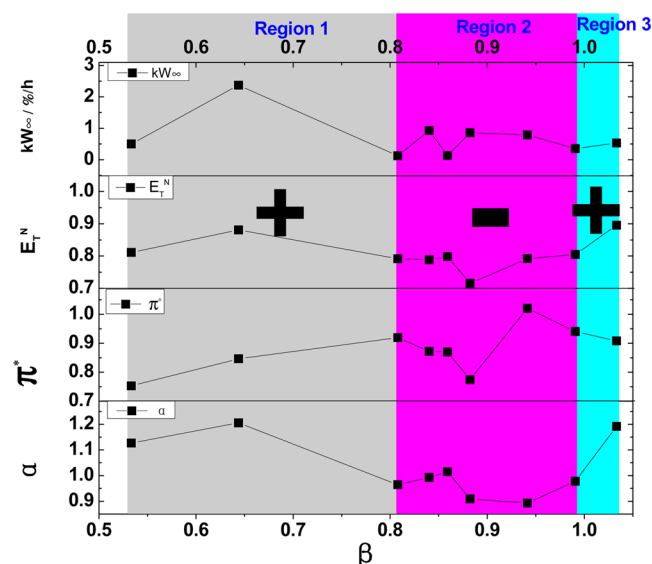


**Figure 7.** Relationship between water sorption initial rate IR ( $kW_{\infty}$ ) and  $E_T^N$ ,  $\alpha$ ,  $\beta$ , and  $\pi^*$  of amino acid ILs.

Results show that  $W_{\infty}$  does not have a direct linear relationship with the four solvatochromic parameters individually (i.e.,  $E_T^N$ ,  $\alpha$ ,  $\beta$ , and  $\pi^*$ ) (Figure 5). However, an interesting finding is that  $W_{\infty}$  has a relationship with  $E_T^N$ , depending on the value of  $\beta$ . Namely,  $W_{\infty}$  is positively related to  $E_T^N$  ( $\beta < 0.8$  or  $0.9 < \beta < 1$ ) and negatively related to  $E_T^N$  ( $0.8 < \beta < 0.9$  or  $1 < \beta$ ) (Figure 5). Four regions exist for this case: region 1 ( $\beta < 0.8$ ), region 2 ( $0.8 < \beta < 0.9$ ), region 3 ( $0.9 < \beta < 1$ ), and region 4 ( $1 < \beta$ ). The relationship could be summarized as “+−+−”. It indicates that  $E_T^N$  (polarity) and  $\beta$  (hydrogen-bonding basicity) have important roles in determining the value of  $W_{\infty}$ .

Note that the complicated relationship (four regions) between  $W_{\infty}$  and  $E_T^N$ ,  $\alpha$ ,  $\beta$ , and  $\pi^*$  might also be due to the discrepancy of the modified two-step water sorption model by which the value of  $W_{\infty}$  was obtained.<sup>17,20,23</sup> The fitting curve for [P<sub>4444</sub>][Lys] within 24 h also displays the non-perfectness of the modified two-step sorption model. Also, the solvatochromic

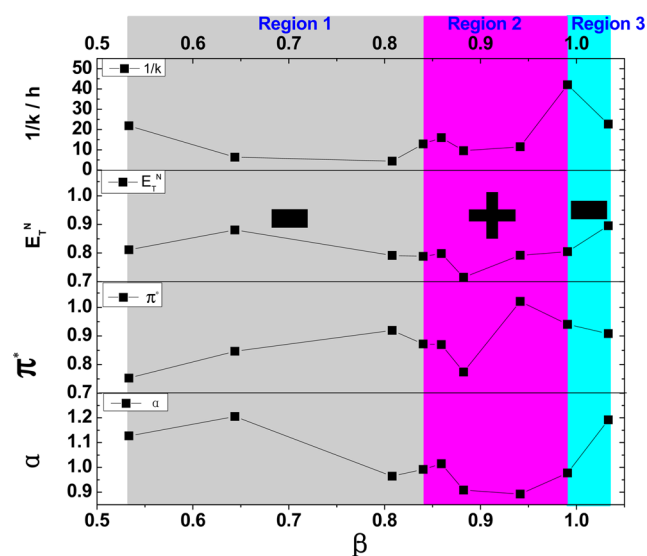


**Figure 8.** Relationship between water sorption difficulty  $D$  ( $1/k$ ) and  $E_T^N$ ,  $\alpha$ ,  $\beta$ , and  $\pi^*$  of amino acid ILs.

parameters for all the amino acid ILs were measured by mixing 3 wt % (mass fraction) water because of the high viscosity of some amino acid ILs investigated (i.e., [MMAEMMIM][Tau]). However, the same relationship is witnessed for average rate (AR), initial rate (IR), and degree of difficulty to reach equilibrium ( $D$ ), which corroborates our conjecture that hygroscopicity is related to  $E_T^N$  within a specific range of  $\beta$ .

**Average Rate of Water Sorption.** Dividing the water sorption capacity within 24 h ( $W_{24h}$ ) by 24 (h) would obtain an average water sorption rate ( $R_{24h}$ ), i.e.,  $R_{24h} = W_{24h}/24$ . The relationship between  $R_{24h}$  and  $E_T^N$ ,  $\alpha$ ,  $\beta$ , and  $\pi^*$  is investigated and shown in Figure 6. The results indicate that  $R_{24h}$  does not have direct linear relationship with the four solvatochromic parameters individually but has a relationship with  $E_T^N$ , depending on the value of  $\beta$ . It is the same as the relationship for  $W_{\infty}$ . But the difference between them is still distinct for the specific relationship.  $R_{24h}$  is positively related to  $E_T^N$  ( $\beta < 0.8$  or  $1 < \beta$ ) and negatively related to  $E_T^N$  ( $0.8 < \beta < 1$ ) (Figure 6). In this case, only three regions appear: region 1 ( $\beta < 0.8$ ), region 2 ( $0.8 < \beta < 1$ ), and region 3 ( $1 < \beta$ ). The relationship could be summarized as “+−+”.

**Initial Rate of Water Sorption.** Initial rate (IR) of water sorption by ILs is often neglected in previous studies; people mainly focus on the saturated water sorption capacity. Actually, the initial water sorption rate is more practical because it can be used to assess the robust water sorption in a limited time period. Thus, we propose the parameter,  $kW_{\infty}$ , to indicate the initial water sorption rate by amino acid ILs, as suggested in the sorption rectangle above (Scheme 3).

The initial rate (IR) of water sorption is indicated by  $kW_{\infty}$ , also derived from the modified two-step sorption model.<sup>17</sup> For the nine amino acid ILs, [P<sub>4444</sub>][Lys] has the highest initial rate, while [P<sub>4444</sub>][Glu] and [aEMMIM][Gly] have the least (Table 3). [P<sub>4444</sub>][Lys] and [P<sub>4444</sub>][Glu] also have the greatest and least water sorption capacity, respectively. Faster water sorption leads to greater water sorption capacity, although they are not necessary linearly correlated.

The relationships between the initial rate ( $kW_{\infty}$ ) and  $E_T^N$ ,  $\alpha$ ,  $\beta$ , and  $\pi^*$  are shown in Figure 7. It is similar to that of water average sorption rate within 24 h,  $R_{24h}$ . Namely,  $kW_{\infty}$  is positively related to  $E_T^N$  ( $\beta < 0.8$  or  $1 < \beta$ ) and negatively



related to  $E_T^N$  ( $0.8 < \beta < 1$ ) (Figure 7). Three regions (i.e., region 1,  $\beta < 0.8$ ; region 2,  $0.8 < \beta < 1$ ; and region 3,  $1 < \beta$ ) could also be summarized as “+–+”. Designing the amino ILs with a higher initial rate or average rate could be done as follows. Step 1: estimating the value of hydrogen-bonding accepting ability  $\beta$ . Step 2: determining to which region the  $\beta$  belongs. Step 3: increasing (decreasing) the polarity in “+” (“–”) region would enhance the initial rate or average rate of water sorption by amino acid ILs. Other kinds of hygroscopicity parameters could also be predicted this way.

**Water Sorption Difficulty.** Water sorption difficulty ( $D$ ) denotes the degree of difficulty for amino acid ILs to reach equilibrium, i.e., steady state. On the basis of the previous study,<sup>17</sup> we used the parameter  $1/k$  to represent the water sorption difficulty. A higher value of  $1/k$  means more time is needed to reach water sorption equilibrium.<sup>17,20,23</sup>

The relationships between water sorption difficulty and the four solvatochromic parameters (i.e.,  $E_T^N$ ,  $\alpha$ ,  $\beta$ , and  $\pi^*$ ) are given in Figure 8. Contrary to that of  $R_{24h}$  and  $kW_\infty$ , they present a “+–+” sequence with  $\beta = 0.85$  and  $\beta = 1$  as the boundary. Note that the range of three regions is slightly different than that of  $R_{24h}$  and  $kW_\infty$ , i.e., region 1 ( $\beta < 0.85$ ), region 2 ( $0.85 < \beta < 1$ ), and region 3 ( $1 < \beta$ ) for  $1/k$ . In regions 1 and 3, a higher value of polarity means that it is easier to reach water sorption equilibrium. However, in region 2, a higher value of polarity of amino acid ILs makes the equilibrium more difficult to reach.

## CONCLUSION

Nine amino acid ILs are found to be highly hygroscopic when exposed to the air for 24 h. Among them,  $[P_{4444}][Lys]$  is the most hygroscopic, while  $[P_{4444}][Glu]$  is the least. The imidazolium-based amino acid ILs are among the hygroscopicity range of phosphonium salts. On the basis of the water sorption experiments, an arrow-shooting ball model was proposed to simulate the interaction mechanism between water and amino acid ILs. Greater ILs–ILs interaction (anion–anion or cation–anion) would lead to less ILs–water (anion–water or cation–water) interaction, hence producing less hygroscopicity. Namely, the golden ball (ILs) with high ILs–ILs interaction is difficult to be penetrated by the arrow (water molecule), hence producing lower hygroscopicity. This golden ball includes two types, i.e., cation–anion golden ball and anion–anion golden ball, where the first type leads to a more hydrophobic effect than the second type. However, a melon ILs ball with weak ILs–ILs interaction could be easily shot through by the water arrow, hence producing high hygroscopicity.

More importantly, the predication of hygroscopicity of nine amino acid ILs were conducted with four solvatochromic parameters, i.e., polarity,  $E_T^N$ ; hydrogen-bonding donating ability,  $\alpha$ ; hydrogen-bonding accepting ability,  $\beta$ ; and dipolarity polarizability,  $\pi^*$ . Results show that hygroscopicity is not directly related to the four solvatochromic parameters individually; however, it is related to  $E_T^N$ , depending on the value of  $\beta$ . Specifically, for saturated water sorption capacity,  $W_\infty$ , it shows a “+–+” symbol. For the degree of difficulty to reach equilibrium, it shows a “–+–” symbol. While for the initial rate,  $kW_\infty$ , and average rate,  $R_{24h}$ , it shows a “+–+” symbol. The symbols “+” and “–” mean that hygroscopicity is positively or negatively related to polarity  $E_T^N$  in a specific region of the hydrogen-bonding accepting ability  $\beta$ . Therefore, the hygroscopicity parameters of amino acid ILs could be predicted and designed by estimating  $\beta$  first, then classifying the

region of  $\beta$ , and finally, determining the hygroscopicity by the  $E_T^N$  according to the corresponding relationship between them.

It should be noted that we only investigated nine amino acid ILs, so the numbers of samples might be limited. Also, the relationship between the hygroscopicity and solvatochromic parameters is a qualitative analysis rather than a quantitative analysis. More work needs to be done to make the hygroscopicity of amino acid ILs clearer.

## AUTHOR INFORMATION

### Corresponding Author

\*Tel.: +86-10-62514925. Fax: +86-10-62516444. E-mail: tcmu@chem.ruc.edu.cn.

### Notes

The authors declare no competing financial interest.

## ACKNOWLEDGMENTS

This work was supported by the National Natural Science Foundation of China (21173267), the Fundamental Research Funds for the Central Universities, and the Research Funds of Renmin University of China (12XNLL05).

## REFERENCES

- (1) Chen, Y.; Cao, Y.; Shi, Y.; Xue, Z.; Mu, T. Quantitative research on the vaporization and decomposition of  $[EMIM][Tf_2N]$  by thermogravimetric analysis–mass spectrometry. *Ind. Eng. Chem. Res.* **2012**, *51* (21), 7418–7427.
- (2) Wang, C.; Luo, X.; Luo, H.; Jiang, D.; Li, H.; Dai, S. Tuning the basicity of ionic liquids for equimolar  $CO_2$  capture. *Angew. Chem., Int. Ed.* **2011**, *50* (21), 4918–4922.
- (3) Ren, S.; Hou, Y.; Tian, S.; Chen, X.; Wu, W. What are functional ionic liquids for the absorption of acidic gases? *J. Phys. Chem. B* **2013**, *117* (8), 2482–2486.
- (4) Zhang, X.; Dong, H.; Zhao, Z.; Zhang, S.; Huang, Y. Carbon capture with ionic liquids: Overview and progress. *Energy Environ. Sci.* **2012**, *5* (5), 6668–6681.
- (5) Chen, Q.; Xu, A.; Li, Z.; Wang, J.; Zhang, S. Influence of anionic structure on the dissolution of chitosan in 1-butyl-3-methylimidazolium-based ionic liquids. *Green Chem.* **2011**, *13* (12), 3446–3452.
- (6) Ohno, H.; Fukumoto, K. Amino acid ionic liquids. *Acc. Chem. Res.* **2007**, *40* (11), 1122–1129.
- (7) Kagimoto, J.; Fukumoto, K.; Ohno, H. Effect of tetrabutylphosphonium cation on the physico-chemical properties of amino–acid ionic liquids. *Chem. Commun.* **2006**, *0* (21), 2254–2256.
- (8) Tao, G. H.; He, L.; Liu, W. S.; Xu, L.; Xiong, W.; Wang, T.; Kou, Y. Preparation, characterization and application of amino acid-based green ionic liquids. *Green Chem.* **2006**, *8* (7), 639–646.
- (9) Rong, H.; Li, W.; Chen, Z.; Wu, X. Glutamic acid cation based ionic liquids: Microwave synthesis, characterization, and theoretical study. *J. Phys. Chem. B* **2008**, *112* (5), 1451–1455.
- (10) Xue, Z.; Zhang, Z.; Han, J.; Chen, Y.; Mu, T. Carbon dioxide capture by a dual amino ionic liquid with amino–functionalized imidazolium cation and taurine anion. *Int. J. Greenhouse Gas Control* **2011**, *5* (4), 628–633.
- (11) Zhang, S. J.; Zhang, J. M.; Dong, K.; Zhang, Y. Q.; Shen, Y. Q.; Lv, X. M. Supported absorption of  $CO_2$  by tetrabutylphosphonium amino acid ionic liquids. *Chem.—Eur. J.* **2006**, *12* (15), 4021–4026.
- (12) Ohira, K.; Yoshida, K.; Hayase, S.; Itoh, T. Amino acid ionic liquid as an efficient cosolvent of dimethyl sulfoxide to realize cellulose dissolution at room temperature. *Chem. Lett.* **2012**, *41* (9), 987–989.
- (13) Muhammad, N.; Man, Z.; Bustam, M. A.; Mutalib, M. I. A.; Wilfred, C. D.; Rafiq, S. Dissolution and delignification of bamboo biomass using amino acid-based ionic liquid. *Appl. Biochem. Biotechnol.* **2011**, *165* (3–4), 998–1009.

- (14) Kroupa, D. M.; Brown, C. J.; Heckman, L. M.; Hopkins, T. A. Chiroptical study of chiral discrimination by amino acid based ionic liquids. *J. Phys. Chem. B* **2012**, *116* (16), 4952–4958.
- (15) He, Y. H.; Hu, Y.; Guan, Z. Natural alpha-amino acid L-lysine-catalyzed Knoevenagel condensations of alpha,beta-unsaturated aldehydes and 1,3-dicarbonyl compounds. *Synth. Commun.* **2011**, *41* (11), 1617–1628.
- (16) Cai, Y.; Peng, Y.; Song, G. Amino-functionalized ionic liquid as an efficient and recyclable catalyst for Knoevenagel reactions in water. *Catal. Lett.* **2006**, *109* (1–2), 61–64.
- (17) Cao, Y.; Chen, Y.; Sun, X.; Zhang, Z.; Mu, T. Water sorption in ionic liquids: kinetics, mechanisms and hydrophilicity. *Phys. Chem. Chem. Phys.* **2012**, *14* (33), 12252–12262.
- (18) Seddon, K. R.; Stark, A.; Torres, M. J. Influence of chloride, water, and organic solvents on the physical properties of ionic liquids. *Pure Appl. Chem.* **2000**, *72* (12), 2275–2287.
- (19) Cammarata, L.; Kazarian, S.; Salter, P.; Welton, T. Molecular states of water in room temperature ionic liquids. *Phys. Chem. Chem. Phys.* **2001**, *3* (23), 5192–5200.
- (20) Cao, Y.; Chen, Y.; Lu, L.; Xue, Z.; Mu, T. Water sorption in functionalized ionic liquids: kinetics and intermolecular interactions. *Ind. Eng. Chem. Res.* **2013**, *52* (5), 2073–2083.
- (21) Tran, C. D.; Lacerda, S. H. D.; Oliveira, D. Absorption of water by room-temperature ionic liquids: Effect of anions on concentration and state of water. *Appl. Spectrosc.* **2003**, *57* (2), 152–157.
- (22) Di Francesco, F.; Calisi, N.; Creatini, M.; Melai, B.; Salvo, P.; Chiappe, C. Water sorption by anhydrous ionic liquids. *Green Chem.* **2011**, *13* (7), 1712–1717.
- (23) Chen, Y.; Cao, Y.; Lu, X.; Zhao, C.; Yan, C.; Mu, T. Water sorption in protic ionic liquids: Correlation between hygroscopicity and polarity. *New J. Chem.* **2013**, *37* (7), 1959–1967.
- (24) Arellano, I. H. J.; Guarino, J. G.; Paredes, F. U.; Arco, S. D. Thermal stability and moisture uptake of 1-alkyl-3-methylimidazolium bromide. *J. Therm. Anal. Calorim.* **2011**, *103* (2), 725–730.
- (25) Cuadrado-Prado, S.; Dominguez-Perez, M.; Rilo, E.; Garcia-Garabal, S.; Segade, L.; Franjo, C.; Cabeza, O. Experimental measurement of the hygroscopic grade on eight imidazolium based ionic liquids. *Fluid Phase Equilib.* **2009**, *278* (1–2), 36–40.
- (26) Huddleston, J. G.; Visser, A. E.; Reichert, W. M.; Willauer, H. D.; Broker, G. A.; Rogers, R. D. Characterization and comparison of hydrophilic and hydrophobic room temperature ionic liquids incorporating the imidazolium cation. *Green Chem.* **2001**, *3* (4), 156–164.
- (27) Aparicio, S.; Alcalde, R.; Atilhan, M. Experimental and computational study on the properties of pure and water mixed 1-ethyl-3-methylimidazolium L-(+)-lactate ionic liquid. *J. Phys. Chem. B* **2010**, *114* (17), 5795–5809.
- (28) Strechan, A. A.; Paulechka, Y. U.; Kabo, A. G.; Blokhin, A. V.; Kabo, G. J. 1-Butyl-3-methylimidazolium tosylate ionic liquid: Heat capacity, thermal stability, and phase equilibrium of its binary mixtures with water and caprolactam. *J. Chem. Eng. Data* **2007**, *52* (5), 1791–1799.
- (29) Zhang, Q.; Wang, N.; Yu, Z. The hydrogen bonding interactions between the ionic liquid 1-ethyl-3-methylimidazolium ethyl sulfate and water. *J. Phys. Chem. B* **2010**, *114* (14), 4747–4754.
- (30) Zhang, Q.; Wang, N.; Wang, S.; Yu, Z. Hydrogen bonding behaviors of binary systems containing the ionic liquid 1-butyl-3-methylimidazolium trifluoroacetate and water/methanol. *J. Phys. Chem. B* **2011**, *115* (38), 11127–11136.
- (31) Gao, Y.; Zhang, L.; Wang, Y.; Li, H. Probing electron density of H-bonding between cation–anion of imidazolium-based ionic liquids with different anions by vibrational spectroscopy. *J. Phys. Chem. B* **2010**, *114* (8), 2828–2833.
- (32) Li, W.; Zhang, Z.; Han, B.; Hu, S.; Xie, Y.; Yang, G. Effect of water and organic solvents on the ionic dissociation of ionic liquids. *J. Phys. Chem. B* **2007**, *111* (23), 6452–6456.
- (33) Ren, S.; Hou, Y.; Wu, W.; Chen, X.; Fan, J.; Zhang, J. Effect of H<sub>2</sub>O on the desulfurization of simulated flue gas by an ionic liquid. *Ind. Eng. Chem. Res.* **2009**, *48* (10), 4928–4932.
- (34) Fu, D.; Sun, X.; Pu, J.; Zhao, S. Effect of water content on the solubility of CO<sub>2</sub> in the ionic liquid [bmim][PF<sub>6</sub>]. *J. Chem. Eng. Data* **2006**, *51* (2), 371–375.
- (35) Goodrich, B. F.; de la Fuente, J. C.; Gurkan, B. E.; Lopez, Z. K.; Price, E. A.; Huang, Y.; Brennecke, J. F. Effect of water and temperature on absorption of CO<sub>2</sub> by amine-functionalized anion-tethered ionic liquids. *J. Phys. Chem. B* **2011**, *115* (29), 9140–9150.
- (36) Kasahara, S.; Kamio, E.; Ishigami, T.; Matsuyama, H. Amino acid ionic liquid-based facilitated transport membranes for CO<sub>2</sub> separation. *Chem. Commun.* **2012**, *48* (55), 6903–6905.
- (37) Kasahara, S.; Kamio, E.; Ishigami, T.; Matsuyama, H. Effect of water in ionic liquids on CO<sub>2</sub> permeability in amino acid ionic liquid-based facilitated transport membranes. *J. Membr. Sci.* **2012**, *415*–416, 168–175.
- (38) Wang, Z.; Fu, L.; Xu, H.; Shang, Y.; Zhang, L.; Zhang, J. Density, viscosity, and conductivity for the binary systems of water + dual amino-functionalized ionic liquids. *J. Chem. Eng. Data* **2012**, *57* (4), 1057–1063.
- (39) Tong, J.; Hong, M.; Chen, Y.; Wang, H.; Yang, J.-Z. Surface properties of aqueous solutions of amino acid ionic liquids: [C<sub>3</sub>mim][Gly] and [C<sub>4</sub>mim][Gly]. *J. Chem. Eng. Data* **2012**, *57* (8), 2265–2270.
- (40) Wu, C.; Wang, J.; Wang, H.; Pei, Y.; Li, Z. Effect of anionic structure on the phase formation and hydrophobicity of amino acid ionic liquids aqueous two-phase systems. *J. Chromatogr., A* **2011**, *1218* (48), 8587–8593.
- (41) Carrete, J.; Garcia, M.; Rodriguez, J.; Cabeza, O.; Varela, L. Theoretical model for moisture adsorption on ionic liquids: A modified Brunauer–Emmet–Teller isotherm approach. *Fluid Phase Equilib.* **2011**, *301* (1), 118–122.
- (42) Reichardt, C. Polarity of ionic liquids determined empirically by means of solvatochromic pyridinium N-phenolate betaine dyes. *Green Chem.* **2005**, *7* (5), 339–351.
- (43) Kamlet, M. J.; Taft, R. The solvatochromic comparison method. I. The beta-scale of solvent hydrogen-bond acceptor (HBA) basicities. *J. Am. Chem. Soc.* **1976**, *98* (2), 377–383.
- (44) Taft, R.; Kamlet, M. J. The solvatochromic comparison method. 2. The alpha-scale of solvent hydrogen-bond donor (HBD) acidities. *J. Am. Chem. Soc.* **1976**, *98* (10), 2886–2894.
- (45) Kamlet, M. J.; Abboud, J. L.; Taft, R. The solvatochromic comparison method. 6. The pi\* scale of solvent polarities. *J. Am. Chem. Soc.* **1977**, *99* (18), 6027–6038.
- (46) Muldoon, M. J.; Gordon, C. M.; Dunkin, I. R. Investigations of solvent–solute interactions in room temperature ionic liquids using solvatochromic dyes. *J. Chem. Soc., Perkin Trans. 2* **2001**, No. 4, 433–435.
- (47) Carmichael, A. J.; Seddon, K. R. Polarity study of some 1-alkyl-3-methylimidazolium ambient-temperature ionic liquids with the solvatochromic dye, Nile Red. *J. Phys. Org. Chem.* **2000**, *13* (10), 591–595.
- (48) Jessop, P. G.; Jessop, D. A.; Fu, D.; Phan, L. Solvatochromic parameters for solvents of interest in green chemistry. *Green Chem.* **2012**, *14* (5), 1245–1259.
- (49) Shukla, S. K.; Khupse, N. D.; Kumar, A. Do anions influence the polarity of protic ionic liquids? *Phys. Chem. Chem. Phys.* **2012**, *14* (8), 2754–2761.
- (50) Ab Rani, M.; Brant, A.; Crowhurst, L.; Dolan, A.; Lui, M.; Hassan, N.; Hallett, J.; Hunt, P.; Niedermeyer, H.; Perez-Arlandis, J. Understanding the polarity of ionic liquids. *Phys. Chem. Chem. Phys.* **2011**, *13* (37), 16831–16840.
- (51) Aki, S. N. V. K.; Brennecke, J. F.; Samanta, A. How polar are room-temperature ionic liquids? *Chem. Commun.* **2001**, *0* (5), 413–414.
- (52) Welton, T.; Crowhurst, L.; Mawdsley, P. R.; Perez-Arlandis, J. M.; Salter, P. A. Solvent-solute interactions in ionic liquids. *Phys. Chem. Chem. Phys.* **2003**, *5* (13), 2790–2794.
- (53) Khupse, N. D.; Kumar, A. Contrasting thermosolvatochromic trends in pyridinium-, pyrrolidinium-, and phosphonium-based ionic liquids. *J. Phys. Chem. B* **2009**, *114* (1), 376–381.

(54) Wu, Y.; Sasaki, T.; Kazushi, K.; Seo, T.; Sakurai, K. Interactions between spiropyrans and room-temperature ionic liquids: Photochromism and solvatochromism. *J. Phys. Chem. B* **2008**, *112* (25), 7530–7536.

(55) Zhao, D.; Wang, J.; Zhou, E. Oxidative desulfurization of diesel fuel using a Brønsted acid room temperature ionic liquid in the presence of H<sub>2</sub>O<sub>2</sub>. *Green Chem.* **2007**, *9* (11), 1219–1222.

(56) Hauru, L. K.; Hummel, M.; King, A. W.; Kilpeläinen, L.; Sixta, H. Role of solvent parameters in the regeneration of cellulose from ionic liquid solutions. *Biomacromolecules* **2012**, *13* (9), 2896–2905.

(57) Doherty, T. V.; Mora-Pale, M.; Foley, S. E.; Linhardt, R. J.; Dordick, J. S. Ionic liquid solvent properties as predictors of lignocellulose pretreatment efficacy. *Green Chem.* **2010**, *12* (11), 1967–1975.

(58) Carvalho, P. J.; Coutinho, J. A. The polarity effect upon the methane solubility in ionic liquids: a contribution for the design of ionic liquids for enhanced CO<sub>2</sub>/CH<sub>4</sub> and H<sub>2</sub>S/CH<sub>4</sub> selectivities. *Energy Environ. Sci.* **2011**, *4* (11), 4614–4619.

(59) Palgunadi, J.; Hong, S. Y.; Lee, J. K.; Lee, H.; Lee, S. D.; Cheong, M.; Kim, H. S. Correlation between hydrogen bond basicity and acetylene solubility in room temperature ionic liquids. *J. Phys. Chem. B* **2011**, *115* (5), 1067–1074.

(60) Zhang, S.; Chen, Z.; Qi, X.; Deng, Y. Distinct influence of the anion and ether group on the polarity of ammonium and imidazolium ionic liquids. *New J. Chem.* **2012**, *36* (4), 1043–1050.

(61) Ficke, L. E.; Brennecke, J. F. Interactions of ionic liquids and water. *J. Phys. Chem. B* **2010**, *114* (32), 10496–10501.

(62) Zhang, L.; Xu, Z.; Wang, Y.; Li, H. Prediction of the solvation and structural properties of ionic liquids in water by two-dimensional correlation spectroscopy. *J. Phys. Chem. B* **2008**, *112* (20), 6411–6419.